magnetochemistry

MDPI

Perspective

Designing Magnetic NanoMOFs for Biomedicine: Current Trends and Applications

Mariangela Oggianu [1,2], Noemi Monni [1,2], Valentina Mameli [1,2], Carla Cannas [1,2], Suchithra Ashoka Sahadevan [1] and Maria Laura Mercuri [1,2,*]

[1] Department of Chemical and Geological Sciences, University of Cagliari, Highway 554, Crossroads for Sestu, I-09042 Monserrato (CA), Italy; mari.oggianu@gmail.com (M.O.); noemi.monni@unica.it (N.M.); valentina.mameli.87@gmail.com (V.M.); ccannas@unica.it (C.C.); suchithraiiserk@gmail.com (S.A.S.)

[2] National Interuniversity Consortium of Materials Science and Technology, INSTM, Street Giuseppe Giusti, 9, I-50121 Florence, Italy

* Correspondence: mercuri@unica.it

Received: 30 July 2020; Accepted: 28 August 2020; Published: 1 September 2020

Abstract: Metal–organic frameworks (MOFs) have shown a great potential in biomedicine due to their promising applications in different fields, including drug delivery, thermometry, theranostics etc. In this context, the development of magnetic sub-micrometric or nanometric MOFs through miniaturization approaches of magnetic MOFs up to the nanoscale still represents a crucial step to fabricate biomedical probes, especially in the field of theranostic nanomedicine. Miniaturization processes have to be properly designed to tailor the size and shape of particles and to retain magnetic properties and high porosity in the same material, fundamental prerequisites to develop smart nanocarriers integrating simultaneously therapeutic and contrast agents for targeted chemotherapy or other specific clinical use. An overview of current trends on the design of magnetic nanoMOFs in the field of biomedicine, with particular emphasis on theranostics and bioimaging, is herein envisioned.

Keywords: metal–organic frameworks; magnetism; biomedical applications; theranostics; biocompatibility; nanoMOFs

1. Introduction

Metal–organic frameworks (MOFs) are crystalline porous compounds formed by the self-assembling of metal ions and organic linkers [1–3]. Due to the possibility to tailor their composition by a proper choice of metal ions [4] and organic linkers, it can be possible to develop MOFs with applications in many areas, such as catalysis, sensing, gas-separation/adsorption/detection, information storage and telecommunications [5–15]. Furthermore, the possibility to miniaturize MOFs up to the nanoscale level, nanoMOFs, makes them interesting candidates in biomedicine due to their unique chemical and physical properties, i.e., high surface area, easy to functionalize and large pore sizes [16]. Here, the term nanoMOFs is used both for nanoparticles (with size up to 100 nm) and sub-micrometric particles (commonly with size lower than 300–400 nm). NanoMOFs could be a promising alternative to their inorganic (metals, silica [17], zeolites [18], ferrites [19–22]) and organic (micelles, micro-emulsions, liposomes and polymers) counterparts, already proposed for biomedical applications [23], and they are excellent candidates to be used in drug delivery, nanothermometry, biosensing, bioimaging and as magnetic resonance imaging (MRI) contrast agents [24–26]. An overview of their applications in nanomedicine is reported in Figure 1. Among these applications, theranostics is widely explored due to its capability to combine specific targeted therapy and diagnostic imaging to treat and monitor simultaneously different kind of diseases with minimal side effect [27]. In 2010, Lin and co-workers demonstrated the successful use of magnetic nanoMOFs in the theranostics field [12], pointing out

that magnetism is a fundamental pre-requirement of a material to act as a suitable theranostic probe. Furthermore the construction of hybrid composite systems by combining nanoMOFs with inorganic nanoparticles [28] is a valuable strategy for developing biomedical probes, especially in theranostics [20]. Magnetic MOFs can be obtained by self-assembling both paramagnetic metals and/or open-shell organic linkers etc. [29–32], giving rise to a porous magnet. Recently, Coronado et al. [33] highlighted the crucial role of chemical design in developing these materials, pointing out that exchange magnetic interactions require short distances between metal centers (the spin carriers), while to achieve high porosity, long linkers are often employed, although detrimental for magnetic ordering. An outlook on (i) design and synthetic approaches for developing magnetic sub-micrometric or nanometric MOFs, through miniaturization of the corresponding bulk MOFs, and (ii) their applications as valuable theranostic smart nanocarriers, integrating simultaneously therapeutic and contrast agents for targeted chemotherapy, is herein provided. Key systems are discussed as perspective, in order to highlight the paramount importance of these multifunctional nanoplatforms in cancer and antibacterial therapy treatment and monitoring, focusing on drug delivery and MRI.

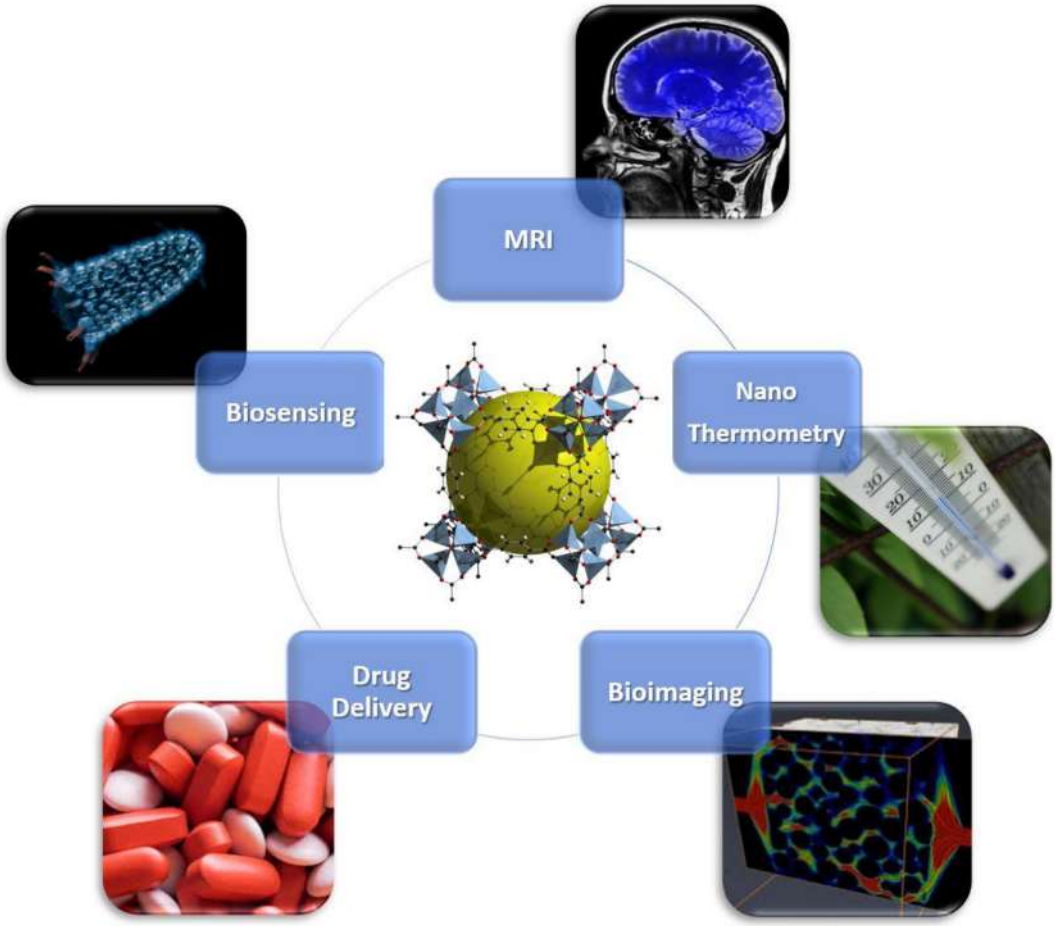

Figure 1. Overview of biomedical Applications of nanometal–organic frameworks (nanoMOFs). Bioimaging is licensed under the Creative Commons Attribution 3.0 License (https://creativecommons.org/licenses/by/3.0/); biosensing is also licensed under the Creative Commons Attribution-Share Alike 3.0 Unported license (https://creativecommons.org/licenses/by-sa/3.0/deed.en); MRI, drug delivery and nanothermometry are royalty-free.

2. Biocompatible MOF Design

The use of biocompatible MOFs, in nanomedicine, requires a proper chemical design, and the choice of the metal ion is crucial for the specific application. Paramagnetic metals, in particular those

of first row transition series i.e., Cr^{III}, Mn^{II}, Fe^{II}/Fe^{III}, Co^{II}, Ni^{II} and Cu^{II}, are widely employed as suitable nodes for obtaining magnetic MOFs, and the most appropriate metals are Mn^{II} and Fe^{III}, for d-transition metal ions and Gd^{III} for lanthanides. In Table 1, magnetic properties and biomedical applications of the most used d-/f-transition metal ions for constructing magnetic MOFs are reported.

Table 1. Magnetic moments, ionic radii, LMedian Lethal Dose (D_{50}) and biomedical applications of magnetic MOF nodes.

Metal Ion	Magnetic Moment (μ)	Ionic Radius (pm)	LD_{50}	Biomedical Application	References
Cr^{III}	3 μ_B	69	-	Drug delivery	[34,35]
Mn^{II}	5 μ_B	80	1.5 g/kg	Contrast agent MRI	[35–37]
Fe^{II}	4 μ_B	83	30 g/kg	CT imaging, optical imaging	[35,36,38]
Fe^{III}	5 μ_B	63	30 g/kg	Drug delivery, optical imaging	[16,35,36,39]
Co^{II}	3 μ_B	72	-	Biosensors, bactericidal agents	[35,40]
Ni^{II}	2 μ_B	69	-	Drug delivery	[35,41]
Cu^{II}	1 μ_B	72	25 μg/kg	Drug delivery	[35,36,42,43]
Gd^{III}	8 μ_B	94	58.2 μM (LC_{50})	Contrast agent MRI	[35,44–46]

Organic linkers are selected taking into account (i) their capability to favor both exchange magnetic interactions between metal ions and large pores to enable drug encapsulation and (ii) their biocompatibility [47,48]. There are a wide variety of organic linkers that may act as building blocks for the design of biofriendly MOFs, such as amino acids, peptides, proteins, nucleobases, phosphonic acids and carboxylic acids [36,49,50], reported in Scheme 1. The MIL (Materials of Institute Lavoisier) and UIO (University of Oslo) classes (vide infra), based on polycarboxylates ligands, are the most commonly used in biomedicine. Phosphonates, sulfonates, imidazolates, amines, pyridyl, phenolates are also valuable linkers [51].

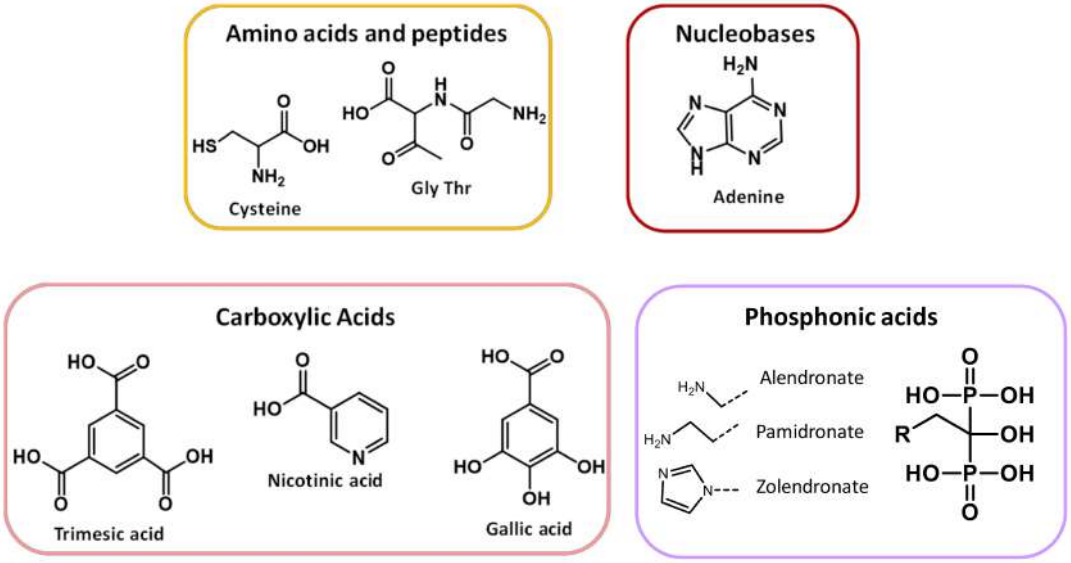

Scheme 1. Biofriendly linkers used to prepare BioMOFs.

3. Miniaturization

The applications of MOFs depend on their size: bulk MOFs with micrometer size are generally employed for catalysis, gas storage and separation. Conversely, nanoMOFs are commonly used in biomedicine, particularly in drug delivery and sensing, due to their tunable structures and high

porosity. Indeed, as for inorganic nanoparticles, size, shape, and surface functionalization of the nanoMOFs are crucial properties to be controlled for biomedical applications. A controlled fine-tuning of MOF size is an essential requirement for their biological activity since biodistribution, cellular uptake and body excretion processes are strictly size dependent. Furthermore, the smaller the MOF size, the more penetration ability into cellular membranes. In particular, crossing biological barriers, clearance from circulation by the reticulo endothelial system (RES) and filtering processes are size related, depending on the different classes of involved blood capillaries [52]. Cell uptake occurs via endocytosis for species <0.5 μm or via phagocytosis for species >0.5 μm. Moreover, in the case of inorganic nanoparticles, systems with size lower than 50–100 nm are easily trapped in the hepatic parenchyma or filtered by kidneys; if larger than 200 nm, they are filtered in the liver or in the spleen; but for sizes larger than 4 μm, they are blocked in the lungs [48,52]. Further aspects need to be taken into account when cancer cells are the target in drug delivery, i.e., the tissue oxygenation and nutrition levels, pH and enhanced permeation and retention (EPR) effects [21,52]. Moreover, the shape of nanoparticle as well as their size renders this scenario more complex. Finally, a proper functionalization of nanoparticles surface might be responsible for effective circulation times, targeting, avoiding opsonization, aggregation/agglomeration phenomena, and chemical/colloidal stability [48,52].

With this view, downsizing MOFs to the nanoscale is also a pre-requirement to exploit applications in biomedicine [53]. Therefore, for nanoparticles [54–56], the synthetic strategy plays a key role in size and shape tailoring. Although for inorganic nanoparticles promising results in terms of size and shape homogeneities can be obtained via surfactant-assisted thermal decomposition of organic complexes and solvothermal methods [55,57,58], efficient MOF miniaturization methods are still in their infancy. Detailed characterization studies on the mechanism of nanoMOF formation processes evidenced that nucleation and growth processes, commonly, follow the LaMer and Dinegar model [58,59] for inorganic nanoparticles [60]. According to this mechanism, a rapid nucleation should be followed by a separate growth in order to obtain low-dispersity and size-selected products. Very recently, Wang et al. [61] developed a method aimed to achieve size-control, from the nano- to the sub-micrometric range size, in the synthesis of nine nanoMOFs (HKUST-1 (Hong Kong University of Science and Technology-1); MIL (Materials of Institute Lavoisier)-101(Fe), MIL-101-NH_2(Fe), MIL-100(Fe), ZIF (Zeolitic Imidazolate Framework); UiO (University of Oslo)-8, MOF-801, ZIF-90, ZIF-67, and UIO-66(Zr)), by controlling the supersaturation degree of reactions. The selected nanoMOFs, i.e., MIL-101(Fe), b) MIL-100(Fe), ZIF-8, MOF-801, ZIF-67, UIO-66-(Zr), representative of different sizes and shapes, are reported in Figure 2.

In particular, they separately delivered metal and ligand stock solutions at a controlled feed rate. NanoMOFs are usually prepared by hydro/solvothermal methods, reverse microemulsion, microwave-assisted, sonochemical methods, and ball milling and reviews on these methods are reported in the literature [48,53,58]. The methods have been led back to three general strategies: (i) rapid nucleation, (ii) confinement within a nanoreactor, and/or (iii) coordination regulation by proper metal–ligand interactions [57]. Interestingly, a targeting strategy based on the pH-induced aggregation of the MIL-100(Fe) nanoMOF was proposed by Simon-Yarza et al. for lung tissues [62], which demonstrates the key role of aggregation/agglomeration phenomena in biomedical applications also for magnetic nanoMOFs as for magnetic nanoparticles. Besides size-related research, studies on nanoMOF morphology and surface functionalization [63–68] are also reported in the literature.

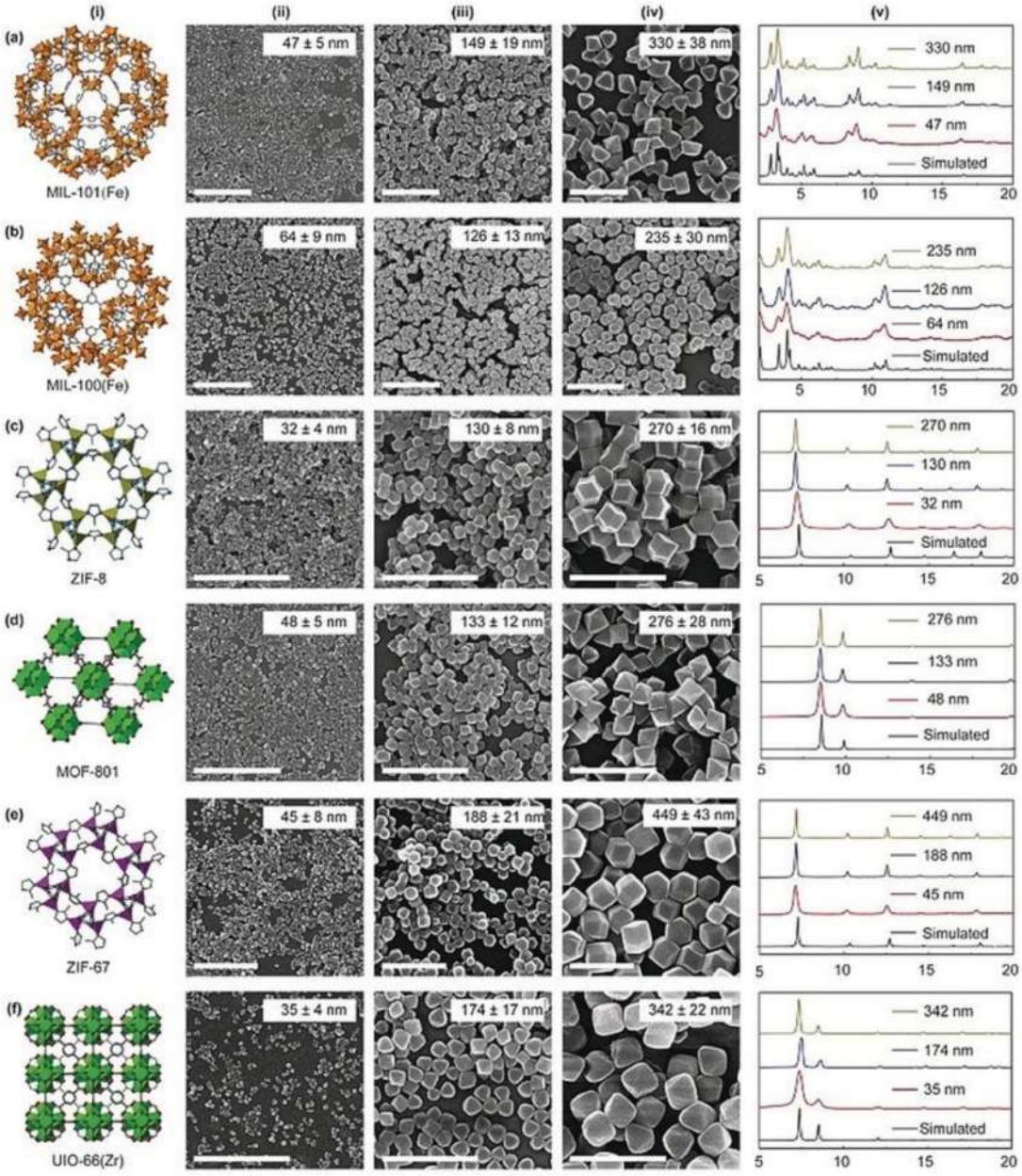

Figure 2. (**i**): (**a**) MIL-101(Fe); (**b**) MIL-100(Fe); (**c**) ZIF-8. (**d**) MOF-801; (**e**) ZIF-67. (**f**) UIO-66-(Zr). (**ii**)–(**iv**) images of representative nanoMOFs of different sizes. Scale bar: 1 μm. (**v**) Simulated and experimental PXRD (Powder X-Ray Diffraction) patterns of different sized nanoMOFs. Reprinted with permission from [61], Copyright 2020 from John Wiley & Sons, Inc. (Hoboken, NJ, USA).

4. Magnetic MOF Applications

Figure 3 summarizes the specific theranostic abilities, i.e., multimodal imaging capability and combined chemo-photothermal therapy, required to develop a promising next-generation class of theranostic nanoagents for FOI (Fluorescence Optical Imaging) and MRI along with synchronous, efficient and safe (low-toxicity) cancer therapy. Key examples of nanosystems showing these features are discussed below.

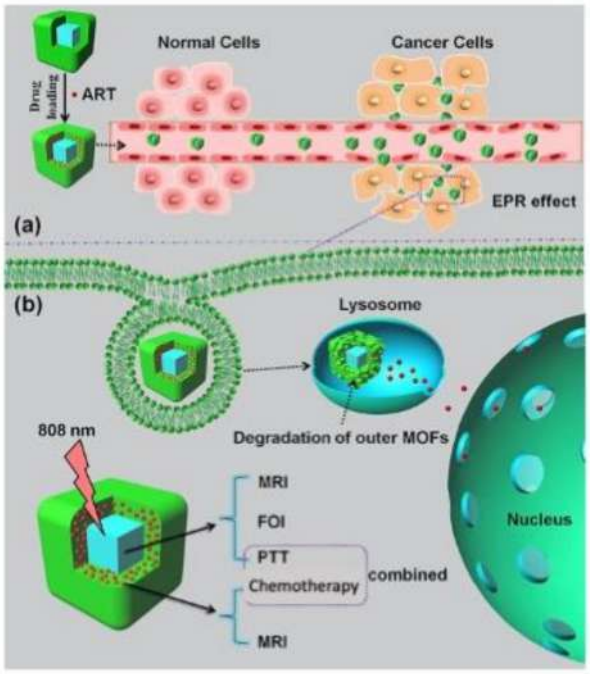

Figure 3. Picture of multifunctional nanoMOFs targeting tumors for combined therapy. (**a**) Loading and delivery process through the enhanced permeation and retention (EPR) effect. (**b**) pH-responsive degradation of outer magnetic nanoMOFs for drug release and dual-modal FOI- and MRI-guided cancer therapy in vitro and in vivo. Reprinted with permission from [69], copyright 2020 from Elsevier (Amsterdam, The Netherlands).

4.1. Gd^{III}-Based MOFs

The majority of paramagnetic gadolinium-based complexes are used as therapeutic agents and/or contrast agents in theranostics due to (i) a large shortening of the longitudinal relaxation time (T1), which, being dominant in tissues respect to the transverse one, enhances the contrast by maximizing signal intensity, and (ii) high longitudinal relaxivity (R1), a quantitative change in relaxation rate of the water protons after addition of the contrast agents [70]. Nanoscaled gadolinium MOFs are even more versatile agents for clinical use due to the combination of gadolinium magnetic properties to drug uptake, due to high porosity, providing valuable nanoplatforms with multiple functionalities i.e., therapeutic, contrast and biomolecular specific-targeting abilities.

Recently, Boyes's et al. fabricated a nanoscaled Gd^{III} MOF theranostics system, formed by nanoparticles with a 20–25 nm average width and a 100–150 nm length, functionalized via a reversible addition–fragmentation chain transfer (RAFT,) with poly(*N*-isopropylacrylamide)-co -poly(*N*-acryloxysuccinimide)-co-poly(fluorescein-*O*-methacrylate) (PNIPAM-co-PNAOS-co-PFMA), which is used as scaffold for the attachment of methotraxate, as a chemotherapeutic agent, and H-glycine-arginine-glycine-aspartate-serine-NH_2 peptide as a targeting ligand for biomolecular recognition. A Gd^{III} MOF nanoparticle, functionalized with PNIPAM-co-PNAOS-co-PFMA biocompatible polymer, showing a functional group for attachment (RAFT), a reactive side chain, a fluorescent tag, a therapeutic agent and a targeting ligand for biomolecular recognition, is reported in Figure 4. This multifunctional magnetic nanocarrier is biocompatible and shows, in vitro cancer cell targeting, bimodal imaging and disease treatment capabilities, preserving a good performance of each individual unit [71].

Very recently, Yin et al. proposed a challenging strategy to fabricate a smart biocompatible nanoplatform for in vivo MRI-guided, pH-responsive precision chemotherapy. Nanoscaled Gd^{III} MOFs, with a spherical shape and a 182 nm hydrodynamic size, were obtained by self-assembling Gd^{III} chloride and 5-boronobenzene-1,3-dicarboxylic acid (BBDC) in a dimethylsulfoxide/water solution.

After doxorubicin (DOX) loading and surface functionalization with glucose via a diol-borate reversible reaction, a versatile DOX@Gd-MOF-Glu composite was obtained, acting as multifunctional theranostic nanocarrier. The wise choice of BBDC as a functional ligand allowing for glucose coating increases simultaneously biocompatibility, specific tumor-targeting and DOX delivery capabilities [72], as well as high values of T1 relaxivity. A novel type of nanoscaled Gd^{III}-porphyrin MOF with folic acid (FA) was obtained, showing nanoparticles of spherical shape with an average diameter of 200 nm. This system can be used for image-guided treatment of hepatocellular carcinoma (HCC). In fact, FA is able to target the active tumor and select the entry in tumor cells while porphyrin, showing impressive emission properties, acting as a theranostics platform for both fluorescence-guided imaging and PDT (Photodynamic Therapy) [73]. These Gd^{III} MOFs show relaxivities considerably higher than traditional Gd^{III}-based complexes and, due to their higher molecular weights, show an increase in the enhanced permeability and retention effect. These results together make this multimodal imaging approach suitable to guide cancer therapy in clinical exams.

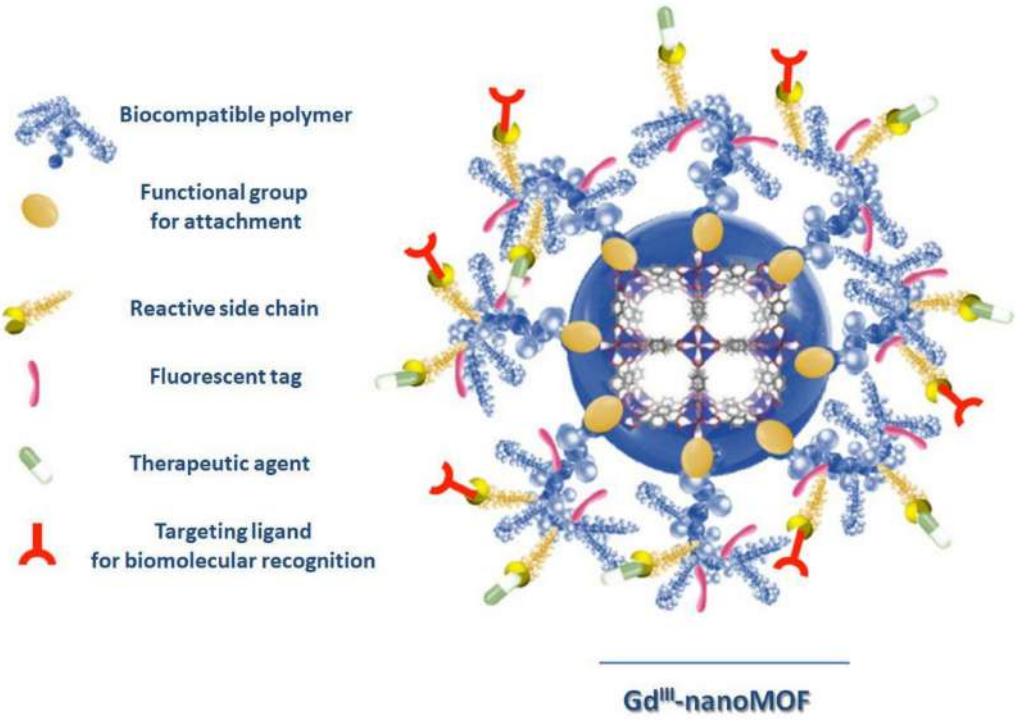

Figure 4. Image of a polymer-functionalized Gd^{III} MOF nanoparticle (shown in the middle) as a biomolecular nanocarrier for targeted imaging and cancer treatment. (Redrawn from [66], copyright 2020 from American Chemical Society, Washington, DC, USA).

4.2. Fe^{III}-Based MOFs

Nanoscaled Gd^{III} MOFs based on carboxylate linkers can go through a degradation of carboxylates in vivo, with the consequent leaking of Gd^{III} in the human body, which may cause nephrogenic systemic fibrosis (NSF) in patients. To overcome Gd^{III} leaking, the MIL systems, i.e., carboxylate-Fe^{III}-based MOFs, can be used due to their lower toxicity of Fe^{III} vs. Gd^{III} metal ions, high porosity, water stability, biodegradability and biocompatibility. Furthermore, their in vivo MRI capabilities along with their efficiency in loading various antitumoral drugs make them promising candidates for clinical use in theranostics [74]. Commonly, high drug doses are essential in chemotherapy to compensate the low biodistribution, but due to the higher side effects, drug delivery systems (DDSs) are a valid approach to overcome this issue. In this regard, MIL-101(Fe) surface functionalization with a modified β-cyclodextrin, via the one-pot post-synthetic "green" method, yields multifunctional nanoscaled MIL-101 -N_3(Fe), showing a 100–200 nm diameter range, capable of simultaneously targeting and

releasing the DOX therapeutic agent at the local level. Notably, MIL-101 -N_3(Fe) nanoparticles with this size can be internalized by cells through both mechanisms of receptor-mediated endocytosis and the enhanced permeability and retention (EPR) effect, while the latter is generally preferred for a diameter up to 400 nm. The benzoic imine and disulfide bonds, formed on functionalized nanoparticle surfaces, provoke a pH and redox response, respectively, showing an enhancement of tumor cell uptake due to the acidic environment and tumor-triggered drug release, both in vitro and in vivo [75]. A novel nanocarrier for image-guided antibacterial therapy was developed based on MIL-100 (Fe) nanoparticles (average diameter ~ 120 nm) loaded with 3-azido-D-alanine (D-AzAla) [76]. The high production of H_2O_2 in the inflammatory environment led to nanoMOF degradation and effective release of D-AzAla into bacteria-infected tissues over time. The delivery performance of D-AzAla@MIL-100 (Fe) NPs was monitored via fluorescence imaging by lightening them up with dibenzocyclooctyne (DBCO-Cy_5) modified through click chemistry. The present nanoMOF-assisted strategy revealed to be successful for precise and more effective bacteria detecting, with several applications in clinical diagnosis and treatments.

Notably, the hydrodynamic diameter of nanoparticles plays a crucial role in facilitating the renal clearance from the body at a suitable timescale. Liu et al. [77] reported on a peculiar nanoscale coordination polymer formed by Fe^{III}, gallic acid (trihydroxy benzoic acid) and poly(vinylpyrrolidone), showing a small hydrodynamic diameter of 5.3 nm. The obtained nanoparticles integrate diagnostic and therapeutic abilities for pH-sensitive MRI-guided photothermal therapy to inhibit cancer cells growth.

The development of hybrid organic/inorganic multifunctional nanoplatforms, where high porosity and magnetic properties coexist synergistically, is of paramount importance for drug delivery and diagnostic information. When MIL-100 (Fe) is deposited via a layer-by-layer strategy to coat Fe_3O_4@C nanoparticles, a multimodal imaging and magnetic targeting nanoplatform showing a monodisperse spherical shape and uniform size at 190nm is obtained [78]. The obtained nanoparticles are loaded with a semisynthetic product derived from artemisinin, a traditional Chinese anticancer drug, dihydroartemisinin (DHA), which has an anticancer activity as well. When nanoparticles reach the cancer cells, the acidic conditions ensure the nanoMOF degradation and the consequent synchronous release of DHA and Fe^{III} ions. Fe^{III} is converted in Fe^{II} by a ferric reductase, which reacts with released DHA, producing reactive oxygen species that destroy proteins and nucleic acid, inducing cancer cell death. Notably, this pH-responsive nanoplatform, due to the presence of iron cations, can be manipulated through an external magnetic field, like a contrast agent for a specific target. By using Prussian blue (PB) nanocubes instead of magnetite as the inner core, it is possible to fabricate a versatile nanoplatform showing cubic shape and average size of ≅200 nm where artemisinin is loaded. This dual MOF's nanostructure is able to act as a T1-T2 dual-modal MRI contrast agent due to the PB inner core and the outer MIL-100 (Fe) MOF and as a fluorescent optical imaging (FOI) agent due to the presence of PB itself. Remarkably, the strategy to take advantage of unique features of individual MOFs, such as (i) the capability of MIL-100(Fe) to load a high content of artemisinin due to its high surface area, (ii) its pH-responsive release and (iii) inner PB photothermal features, paves the way to develop novel multifunctional nanoplatforms with enhanced efficacy in cancer treatments by combining PTT (Photothermal Therapy) with chemotherapy [69].

4.3. Mn^{II}-Based MOFs

Recently, Mn^{II} MOFs have also been investigated for theranostics since Mn^{II} has five unpaired *3d* electrons, which make it a good T1 contrast agent in MRI. Lin et al. reported on a nitrogen-containing bisphosphonate Mn^{II} MOFs in the form of pegylated nanoparticles coated with 1,2-dioleoyl-sn-glycero-3-phosphocholine (DOPC) and cholesterol, showing a diameter of around 80 nm. This nanoMOF shows a high capacity to load zoledronate, an antitumor therapeutic agent, showing also antiangiogenic effects, demonstrated both in vivo and in vitro, acting as multifunctional nanoplatform capable of delivering the drug to cancer cells and to work as an MRI contrast agent [79]. Taking into account the toxic adverse effects of chemotherapy, a very interesting alternative is proposed

by Yin et al.; they developed a theranostics probe in vivo based on Mn^{II}-porphyrin Zr^{IV} carboxylate nanoMOFs for NO free-radical delivery as a therapeutic agent, showing a high molar extinction coefficient, effective photothermal stability, a spindle shape with a ~224 nm diameter and a surface area of ~1900 m^2/g with a pore volume of ~0.67 cm^3/g. This nanoplatform, integrating MRI-guided, spatiotemporally controllable NO delivery and synergistic PTT, represents a novelty in cancer therapy. The action of paramagnetic Mn^{II} inserted in porphyrin ring provides the nanocomposite a strong T1-weighted MRI contrast ability and high photothermal conversion for efficient PTT. Furthermore, NIR (near-infrared, λ = 808 nm) irradiation of this nanosystem ensures a NO-controlled release and synergic PTT for achieving a one-step more efficient cancer therapy [80].

By combining Mn^{II} ions with a zwitterionic carboxylate ligand (*N*-(4-carboxybenzyl)-(3,5 -dicarboxyl) pyridinium bromide), a novel three-dimensional nanoMOF, with a ~50 nm diameter size (too large to be absorbed by the kidneys), was obtained. The choice of the ligand is strictly related to increasing the nanoMOF solubility and stability in aqueous environments, while the choice of the MOF network is made with the aim of lowering the Mn^{II} toxicity by encapsulating the metal in the nanoparticles. Due to the presence of Mn^{II}, the MOF shows good R1 relaxivities and T1-weighted images, making this nanoMOF particularly useful as an MRI contrast agent for revealing kidney-related pathologies [81].

5. Conclusions

Current trends of magnetic nanoMOFs towards biomedical applications, mainly theranostics, are discussed herein, from the fundamental features of their design, to the synthetic strategy to control the size in the nanoscale and to their applications. A crucial requirement for their use in nanomedicine is biocompatibility, which can be achieved by a careful choice of both metal ions (Mn^{II}, Fe^{III}, Fe^{II} and Gd^{III}) and organic linkers, mainly carboxylate derivatives, and by a proper nanoparticle surface functionalization via biofriendly molecules. Remarkably, the latter represents a challenge since it endows to improve circulation times and targeting to avoid opsonization and aggregation/agglomeration phenomena and to increase chemical/colloidal stability [52]. Furthermore a nanoparticle diameter smaller than 200 nm, with a narrow size-distribution, is preferable since biodistribution, penetration ability into cellular membranes, cellular uptake and body excretion processes require a fine control of MOF nanoparticles size. Considering that the major challenge is to obtain porosity and magnetism in the same nanosystem, a promising strategy is the fabrication of hybrid organic/inorganic nanoplatforms by combing materials with magnetic properties, i.e., magnetic inorganic nanoparticles (magnetite, maghemite, etc.), with highly porous nanoMOFs. However, the development of biofriendly multifunctional stimuli-responsive nanoplatforms that are simultaneously biodegradable and stable in body fluids still remains a challenge in nanomedicine. In conclusion, these nanosystems can be envisaged as potential candidates for magnetic particle imaging (MPI), a comparatively young tomographic technique, complementing magnetic fluid hyperthermia for post-treatment tumor monitoring [78].

Author Contributions: M.O. and N.M. contributed equally in terms of literature searching and paper writing; S.A.S. contributes in accurate literature searching; V.M. and C.C. contributed to miniaturization section in terms of literature searching and paper writing; M.L.M. supervised the perspective article and wrote the paper with help from all the authors. All authors have read and agreed to the published version of the manuscript.

Funding: This work was supported in Italy by (a) Fondazione di Sardegna-Convenzione triennale tra la Fondazione di Sardegna e gli Atenei Sardi, Regione Sardegna-L.R. 7/2007 annualità 2018-DGR 28/21 del 17.05.2015, project F74I19000940007 and (b) Regione Autonoma della Sardegna-Delibera CIPE n. 31 del 20.02.2015 e deliberazione n. 52/36 del 28.10.2015 "Piano Strategico Sulcis", project SULCIS-820947. (c) CESA−RAS-Piano SULCIS (E58C16000080003) are also acknowledged for PhD grant of M.O. PON AIM (PON Ricerca e Innovazione 2014 – 2020-Azione I.2-D.D. n.407 del 27 febbraio 2018 "Attraction and International Mobility", Cult-GeoChim project n. AIM1890410-3) is gratefully acknowledged for financing the fixed-term researcher fellowship of V. M.

Conflicts of Interest: The authors declare no conflict of interest.

References

1. Mendes, R.F.; Almeida Paz, F.A. Transforming metal-organic frameworks into functional materials. *Inorg. Chem. Front.* **2015**, *2*, 495–509. [CrossRef]
2. Silva, P.; Vilela, S.M.F.; Tomé, J.P.C.; Almeida Paz, F.A. Multifunctional metal-organic frameworks: From academia to industrial applications. *Chem. Soc. Rev.* **2015**, *44*, 6774–6803. [CrossRef]
3. Janiak, C.; Vieth, J.K. MOFs, MILs and more: Concepts, properties and applications for porous coordination networks (PCNs). *New J. Chem.* **2010**, *34*, 2366–2388. [CrossRef]
4. Wang, Q.; Astruc, D. State of the Art and Prospects in Metal-Organic Framework (MOF)-Based and MOF-Derived Nanocatalysis. *Chem. Rev.* **2020**, *120*, 1438–1511. [CrossRef]
5. Bünzli, J.C.G.; Eliseeva, S.V. Lanthanide NIR luminescence for telecommunications, bioanalyses and solar energy conversion. *J. Rare Earths* **2010**, *28*, 824–842. [CrossRef]
6. Gascón, V.; Carucci, C.; Jiménez, M.B.; Blanco, R.M.; Sánchez-Sánchez, M.; Magner, E. Rapid In Situ Immobilization of Enzymes in Metal–Organic Framework Supports under Mild Conditions. *ChemCatChem* **2017**, *9*, 1182–1186. [CrossRef]
7. Ashoka Sahadevan, S.; Monni, N.; Oggianu, M.; Abhervé, A.; Marongiu, D.; Saba, M.; Mura, A.; Bongiovanni, G.; Mameli, V.; Cannas, C.; et al. Heteroleptic NIR-Emitting YbIII/Anilate-Based Neutral Coordination Polymer Nanosheets for Solvent Sensing. *ACS Appl. Nano Mater.* **2020**, *3*, 94–104. [CrossRef]
8. Carucci, C.; Bruen, L.; Gascón, V.; Paradisi, F.; Magner, E. Significant Enhancement of Structural Stability of the Hyperhalophilic ADH from Haloferax volcanii via Entrapment on Metal Organic Framework Support. *Langmuir* **2018**, *34*, 8274–8280. [CrossRef] [PubMed]
9. Ashoka Sahadevan, S.; Monni, N.; Abhervé, A.; Marongiu, D.; Sarritzu, V.; Sestu, N.; Saba, M.; Mura, A.; Bongiovanni, G.; Cannas, C.; et al. Nanosheets of Two-Dimensional Neutral Coordination Polymers Based on Near-Infrared-Emitting Lanthanides and a Chlorocyananilate Ligand. *Chem. Mater.* **2018**, *30*, 6575–6586. [CrossRef]
10. Ye, H.Q.; Li, Z.; Peng, Y.; Wang, C.C.; Li, T.Y.; Zheng, Y.X.; Sapelkin, A.; Adamopoulos, G.; Hernández, I.; Wyatt, P.B.; et al. Organo-erbium systems for optical amplification at telecommunications wavelengths. *Nat. Mater.* **2014**, *13*, 382–386. [CrossRef]
11. Lin, R.B.; Li, L.; Zhou, H.L.; Wu, H.; He, C.; Li, S.; Krishna, R.; Li, J.; Zhou, W.; Chen, B. Molecular sieving of ethylene from ethane using a rigid metal–organic framework. *Nat. Mater.* **2018**, *17*, 1128–1133. [CrossRef]
12. Taylor, K.M.L.; Jin, A.; Lin, W. Surfactant-assisted synthesis of nanoscale gadolinium metal-organic frameworks for potential multimodal imaging. *Angew. Chem. Int. Ed.* **2008**, *47*, 7722–7725. [CrossRef] [PubMed]
13. Zhang, X.; Lin, R.B.; Wang, J.; Wang, B.; Liang, B.; Yildirim, T.; Zhang, J.; Zhou, W.; Chen, B. Optimization of the Pore Structures of MOFs for Record High Hydrogen Volumetric Working Capacity. *Adv. Mater.* **2020**, *32*, 1–6. [CrossRef] [PubMed]
14. Zhang, X.; Frey, B.L.; Chen, Y.S.; Zhang, J. Topology-Guided Stepwise Insertion of Three Secondary Linkers in Zirconium Metal-Organic Frameworks. *J. Am. Chem. Soc.* **2018**, *140*, 7710–7715. [CrossRef] [PubMed]
15. Furukawa, H.; Cordova, K.E.; O'Keeffe, M.; Yaghi, O.M. The chemistry and applications of metal-organic frameworks. *Science* **2013**. [CrossRef] [PubMed]
16. Taylor-Pashow, K.M.L.; Della Rocca, J.; Xie, Z.; Tran, S.; Lin, W. Postsynthetic modifications of iron-carboxylate nanoscale metal-organic frameworks for imaging and drug delivery. *J. Am. Chem. Soc.* **2009**, *131*, 14261–14263. [CrossRef] [PubMed]
17. Vivero-Escoto, J.L.; Huxford-Phillips, R.C.; Lin, W. Silica-based nanoprobes for biomedical imaging and theranostic applications. *Chem. Soc. Rev.* **2012**, *41*, 2673–2685. [CrossRef] [PubMed]
18. Rahimi, M.; Ng, E.P.; Bakhtiari, K.; Vinciguerra, M.; Ahmad, H.A.; Awala, H.; Mintova, S.; Daghighi, M.; Bakhshandeh Rostami, F.; De Vries, M.; et al. Zeolite Nanoparticles for Selective Sorption of Plasma Proteins. *Sci. Rep.* **2015**, *5*, 1–12. [CrossRef] [PubMed]
19. Mameli, V.; Musinu, A.; Ardu, A.; Ennas, G.; Peddis, D.; Niznansky, D.; Sangregorio, C.; Innocenti, C.; Thanh, N.T.K.; Cannas, C. Studying the effect of Zn-substitution on the magnetic and hyperthermic properties of cobalt ferrite nanoparticles. *Nanoscale* **2016**, *8*, 10124–10137. [CrossRef]

20. Sanna Angotzi, M.; Musinu, A.; Mameli, V.; Ardu, A.; Cara, C.; Niznansky, D.; Xin, H.L.; Cannas, C. Spinel Ferrite Core-Shell Nanostructures by a Versatile Solvothermal Seed-Mediated Growth Approach and Study of Their Nanointerfaces. *ACS Nano* **2017**, *11*, 7889–7900. [CrossRef]
21. Reddy, L.H.; Arias, J.L.; Nicolas, J.; Couvreur, P. Magnetic nanoparticles: Design and characterization, toxicity and biocompatibility, pharmaceutical and biomedical applications. *Chem. Rev.* **2012**, *112*, 5818–5878. [CrossRef] [PubMed]
22. Sanna Angotzi, M.; Mameli, V.; Cara, C.; Musinu, A.; Sangregorio, C.; Niznansky, D.; Xin, H.L.; Vejpravova, J.; Cannas, C. Coupled hard–soft spinel ferrite-based core–shell nanoarchitectures: Magnetic properties and heating abilities. *Nanoscale Adv.* **2020**. [CrossRef]
23. Zhao, H.; Serre, C.; Dumas, E.; Steunou, N. Functional MOFs as theranostics. *Met. Fram. Biomed. Appl.* **2020**. [CrossRef]
24. Chedid, G.; Yassin, A. Recent trends in covalent and metal organic frameworks for biomedical applications. *Nanomaterials* **2018**, *8*, 916. [CrossRef]
25. Giner-Casares, J.J.; Henriksen-Lacey, M.; Coronado-Puchau, M.; Liz-Marzán, L.M. Inorganic nanoparticles for biomedicine: Where materials scientists meet medical research. *Mater. Today* **2016**, *19*, 19–28. [CrossRef]
26. Lu, J.; Yang, L.; Zhang, W.; Li, P.; Gao, X.; Zhang, W.; Wang, H.; Tang, B. Photodynamic therapy for hypoxic solid tumors via Mn-MOF as a photosensitizer. *Chem. Commun.* **2019**, *55*, 10792–10795. [CrossRef]
27. Janib, S.M.; Moses, A.S.; MacKay, J.A. Imaging and drug delivery using theranostic nanoparticles. *Adv. Drug Deliv. Rev.* **2010**, *62*, 1052–1063. [CrossRef]
28. Ray Chowdhuri, A.; Bhattacharya, D.; Sahu, S.K. Magnetic nanoscale metal organic frameworks for potential targeted anticancer drug delivery, imaging and as an MRI contrast agent. *Dalt. Trans.* **2016**, *45*, 2963–2973. [CrossRef]
29. Kurmoo, M. Magnetic metal–organic frameworks. *Chem. Soc. Rev.* **2009**, *38*, 1353–1379. [CrossRef]
30. Sahadevan, S.A.; Monni, N.; Abhervé, A.; Cosquer, G.; Oggianu, M.; Ennas, G.; Yamashita, M.; Avarvari, N.; Mercuri, M.L. Dysprosium Chlorocyanoanilate-Based 2D-Layered Coordination Polymers. *Inorg. Chem.* **2019**, *58*, 13988–13998. [CrossRef]
31. Sahadevan, S.A.; Abhervé, A.; Monni, N.; Sáenz De Pipaón, C.; Galán-Mascarós, J.R.; Waerenborgh, J.C.; Vieira, B.J.C.; Auban-Senzier, P.; Pillet, S.; Bendeif, E.E.; et al. Conducting Anilate-Based Mixed-Valence Fe(II)Fe(III) Coordination Polymer: Small-Polaron Hopping Model for Oxalate-Type Fe(II)Fe(III) 2D Networks. *J. Am. Chem. Soc.* **2018**, *140*, 12611–12621. [CrossRef] [PubMed]
32. Benmansour, S.; Hernandez-Paredes, A.; Mondal, A.; Lopez Martinez, G.; Canet-Ferrer, J.; Konar, S.; Gomez-Carcia, C. Slow relaxation of the magnetization, reversible solvent exchange and luminescence in 2D anilato-based frameworks. *Chem. Commun.* **2020**. [CrossRef] [PubMed]
33. Mínguez Espallargas, G.; Coronado, E. Magnetic functionalities in MOFs: From the framework to the pore. *Chem. Soc. Rev.* **2018**, *47*, 533–557. [CrossRef] [PubMed]
34. Horcajada, P.; Serre, C.; Maurin, G.; Ramsahye, N.A.; Balas, F.; Vallet-Regí, M.; Sebban, M.; Taulelle, F.; Férey, G. Flexible porous metal-organic frameworks for a controlled drug delivery. *J. Am. Chem. Soc.* **2008**, *130*, 6774–6780. [CrossRef] [PubMed]
35. Huang, S.; Du, P.; Min, C.; Liao, Y.; Sun, H.; Jiang, Y. Poly(1-amino-5-chloroanthraquinone): Highly Selective and Ultrasensitive Fluorescent Chemosensor for Ferric Ion. *J. Fluoresc.* **2013**, *23*, 621–627. [CrossRef]
36. Horcajada, P.; Gref, R.; Baati, T.; Allan, P.K.; Maurin, G.; Couvreur, P.; Férey, G.; Morris, R.E.; Serre, C. Metal-organic frameworks in biomedicine. *Chem. Rev.* **2012**, *112*, 1232–1268. [CrossRef]
37. Yang, Y.; Liu, J.; Liang, C.; Feng, L.; Fu, T.; Dong, Z.; Chao, Y.; Li, Y.; Lu, G.; Chen, M.; et al. Nanoscale Metal-Organic Particles with Rapid Clearance for Magnetic Resonance Imaging-Guided Photothermal Therapy. *ACS Nano* **2016**, *10*, 2774–2781. [CrossRef]
38. Du, T.; Zhao, C.; ur Rehman, F.; Lai, L.; Li, X.; Sun, Y.; Luo, S.; Jiang, H.; Gu, N.; Selke, M.; et al. In Situ Multimodality Imaging of Cancerous Cells Based on a Selective Performance of Fe^{2+}-Adsorbed Zeolitic Imidazolate Framework-8. *Adv. Funct. Mater.* **2017**, *27*. [CrossRef]
39. Anand, R.; Borghi, F.; Manoli, F.; Manet, I.; Agostoni, V.; Reschiglian, P.; Gref, R.; Monti, S. Host-guest interactions in Fe(III)-trimesate MOF nanoparticles loaded with doxorubicin. *J. Phys. Chem. B* **2014**, *118*, 8532–8539. [CrossRef]
40. An, J.; Geib, S.J.; Rosi, N.L. High and selective CO_2 uptake in a cobalt adeninate metal-organic framework exhibiting pyrimidine- and amino-decorated pores. *J. Am. Chem. Soc.* **2010**, *132*, 38–39. [CrossRef]

41. Cattaneo, D.; Warrender, S.J.; Duncan, M.J.; Kelsall, C.J.; Doherty, M.K.; Whitfield, P.D.; Megson, I.L.; Morris, R.E. Tuning the nitric oxide release from CPO-27 MOFs. *RSC Adv.* **2016**, *6*, 14059–14067. [CrossRef] [PubMed]
42. Wei, L.Q.; Chen, Q.; Tang, L.L.; Zhuang, C.; Zhu, W.R.; Lin, N. A porous metal-organic framework with a unique hendecahedron-shaped cage: Structure and controlled drug release. *Dalt. Trans.* **2016**, *45*, 3694–3697. [CrossRef] [PubMed]
43. Sharma, S.; Mittal, D.; Verma, A.K.; Roy, I. Copper-Gallic Acid Nanoscale Metal-Organic Framework for Combined Drug Delivery and Photodynamic Therapy. *ACS Appl. Bio Mater.* **2019**, *2*, 2092–2101. [CrossRef]
44. Hatakeyama, W.; Sanchez, T.J.; Rowe, M.D.; Serkova, N.J.; Liberatore, M.W.; Boyes, S.G. Synthesis of gadolinium nanoscale metal-organic framework with hydrotropes: Manipulation of particle size and magnetic resonance imaging capability. *ACS Appl. Mater. Interfaces* **2011**, *3*, 1502–1510. [CrossRef]
45. Kundu, T.; Mitra, S.; Díaz Díaz, D.; Banerjee, R. Gadolinium(III)-Based Porous Luminescent Metal–Organic Frameworks for Bimodal Imaging. *Chempluschem* **2016**, *81*, 728–732. [CrossRef]
46. Kawano, T. Use of swimming cells of green paramecia for detection of toxic rare earth ions at lethal and sub-lethal concentration. *Adv. Mater. Res.* **2014**, *875–877*, 2229–2237. [CrossRef]
47. Rojas, S.; Devic, T.; Horcajada, P. Metal organic frameworks based on bioactive components. *J. Mater. Chem. B* **2017**, *5*, 2560–2573. [CrossRef]
48. Giménez-Marqués, M.; Hidalgo, T.; Serre, C.; Horcajada, P. Nanostructured metal-organic frameworks and their bio-related applications. *Coord. Chem. Rev.* **2016**, *307*, 342–360. [CrossRef]
49. Wang, L.; Zheng, M.; Xie, Z. Nanoscale metal-organic frameworks for drug delivery: A conventional platform with new promise. *J. Mater. Chem. B* **2018**, *6*, 707–717. [CrossRef]
50. Imaz, I.; Rubio-Martínez, M.; An, J.; Solé-Font, I.; Rosi, N.L.; Maspoch, D. Metal-biomolecule frameworks (MBioFs). *Chem. Commun.* **2011**, *47*, 7287–7302. [CrossRef]
51. Oggianu, M.; Mameli, V.; Monni, N.; Ashoka Sahadevan, S.; Sanna Angotzi, M.; Cannas, C.; Mercuri, M.L. Nanoscaled Metal-Organic Frameworks (Nano-MOFs): Challenges towards Biomedical Applications. *J. Nanosci. Nanotechnol.* **2019**, in press.
52. Krishnan, K.M. Biomedical nanomagnetics: A spin through possibilities in imaging, diagnostics, and therapy. *IEEE Trans. Magn.* **2010**, *46*, 2523–2558. [CrossRef] [PubMed]
53. Zhang, Y.; Yang, L.; Yan, L.; Wang, G.; Liu, A. Recent advances in the synthesis of spherical and nanoMOF-derived multifunctional porous carbon for nanomedicine applications. *Coord. Chem. Rev.* **2019**, *391*, 69–89. [CrossRef]
54. Cushing, B.L.; Kolesnichenko, V.L.; O'Connor, C.J. Recent advances in the liquid-phase syntheses of inorganic nanoparticles. *Chem. Rev.* **2004**, *104*, 3893–3946. [CrossRef]
55. Mameli, V.; Angotzi, M.S.; Cara, C.; Cannas, C. Liquid Phase Synthesis of Nanostructured Spinel Ferrites—A Review. *J. Nanosci. Nanotechnol.* **2019**, *19*, 4857–4887. [CrossRef]
56. Duan, H.; Wang, D.; Li, Y. Green chemistry for nanoparticle synthesis. *Chem. Soc. Rev.* **2015**, *44*, 5778–5792. [CrossRef]
57. Flügel, E.A.; Ranft, A.; Haase, F.; Lotsch, B.V. Synthetic routes toward MOF nanomorphologies. *J. Mater. Chem.* **2012**, *22*, 10119–10133. [CrossRef]
58. Wang, S.; McGuirk, C.M.; d'Aquino, A.; Mason, J.A.; Mirkin, C.A. Metal–Organic Framework Nanoparticles. *Adv. Mater.* **2018**, *30*, 1–14. [CrossRef]
59. Lamer, V.K.; Dinegar, R.H. Theory, Production and Mechanism of Formation of Monodispersed Hydrosols. *J. Am. Chem. Soc.* **1950**, *72*, 4847–4854. [CrossRef]
60. Thanh, N.T.K.; Maclean, N.; Mahiddine, S. Mechanisms of nucleation and growth of nanoparticles in solution. *Chem. Rev.* **2014**, *114*, 7610–7630. [CrossRef]
61. Wang, X.G.; Cheng, Q.; Yu, Y.; Zhang, X.Z. Controlled Nucleation and Controlled Growth for Size Predicable Synthesis of Nanoscale Metal–Organic Frameworks (MOFs): A General and Scalable Approach. *Angew. Chem. Int. Ed.* **2018**, *57*, 7836–7840. [CrossRef] [PubMed]
62. Simon-Yarza, T.; Giménez-Marqués, M.; Mrimi, R.; Mielcarek, A.; Gref, R.; Horcajada, P.; Serre, C.; Couvreur, P. A Smart Metal–Organic Framework Nanomaterial for Lung Targeting. *Angew. Chem. Int. Ed.* **2017**, *56*, 15565–15569. [CrossRef] [PubMed]

63. Wang, S.; Morris, W.; Liu, Y.; McGuirk, C.M.; Zhou, Y.; Hupp, J.T.; Farha, O.K.; Mirkin, C.A. Surface-specific functionalization of nanoscale metal-organic frameworks. *Angew. Chem. Int. Ed.* **2015**, *54*, 14738–14742. [CrossRef] [PubMed]
64. Agostoni, V.; Horcajada, P.; Noiray, M.; Malanga, M.; Aykaç, A.; Jicsinszky, L.; Vargas-Berenguel, A.; Semiramoth, N.; Daoud-Mahammed, S.; Nicolas, V.; et al. A "green" strategy to construct non-covalent, stable and bioactive coatings on porous MOF nanoparticles. *Sci. Rep.* **2015**, *5*, 1–7. [CrossRef]
65. Cutrone, G.; Qiu, J.; Menendez-Miranda, M.; Casas-Solvas, J.M.; Aykaç, A.; Li, X.; Foulkes, D.; Moreira-Alvarez, B.; Encinar, J.R.; Ladavière, C.; et al. Comb-like dextran copolymers: A versatile strategy to coat highly porous MOF nanoparticles with a PEG shell. *Carbohydr. Polym.* **2019**, *223*, 115085. [CrossRef]
66. Bellido, E.; Hidalgo, T.; Lozano, M.V.; Guillevic, M.; Simón-Vázquez, R.; Santander-Ortega, M.J.; González-Fernández, Á.; Serre, C.; Alonso, M.J.; Horcajada, P. Heparin-Engineered Mesoporous Iron Metal-Organic Framework Nanoparticles: Toward Stealth Drug Nanocarriers. *Adv. Healthc. Mater.* **2015**, *4*, 1246–1257. [CrossRef]
67. Mejia-Ariza, R.; Huskens, J. The effect of PEG length on the size and guest uptake of PEG-capped MIL-88A particles. *J. Mater. Chem. B* **2016**, *4*, 1108–1115. [CrossRef]
68. Hidalgo, T.; Giménez-Marqués, M.; Bellido, E.; Avila, J.; Asensio, M.C.; Salles, F.; Lozano, M.V.; Guillevic, M.; Simón-Vázquez, R.; González-Fernández, A.; et al. Chitosan-coated mesoporous MIL-100(Fe) nanoparticles as improved bio-compatible oral nanocarriers. *Sci. Rep.* **2017**, *7*, 1–14. [CrossRef]
69. Wang, D.; Zhou, J.; Chen, R.; Shi, R.; Zhao, G.; Xia, G.; Li, R.; Liu, Z.; Tian, J.; Wang, H.; et al. Controllable synthesis of dual-MOFs nanostructures for pH-responsive artemisinin delivery, magnetic resonance and optical dual-model imaging-guided chemo/photothermal combinational cancer therapy. *Biomaterials* **2016**, *100*, 27–40. [CrossRef]
70. Caravan, P. Strategies for increasing the sensitivity of gadolinium based MRI contrast agents. *Chem. Soc. Rev.* **2006**, *35*, 512–523. [CrossRef]
71. Rowe, M.D.; Tham, D.H.; Kraft, S.L.; Boyes, S.G. Polymer-modified gadolinium metal-organic framework nanoparticles used as multifunctional nanomedicines for the targeted imaging and treatment of cancer. *Biomacromolecules* **2009**, *10*, 983–993. [CrossRef] [PubMed]
72. Zhang, H.; Shang, Y.; Li, Y.H.; Sun, S.K.; Yin, X.B. Smart Metal-Organic Framework-Based Nanoplatforms for Imaging-Guided Precise Chemotherapy. *ACS Appl. Mater. Interfaces* **2019**, *11*, 1886–1895. [CrossRef] [PubMed]
73. Chen, Y.; Liu, W.; Shang, Y.; Cao, P.; Cui, J.; Li, Z.; Yin, X.; Li, Y. Folic acid-nanoscale gadolinium-porphyrin metal-organic frameworks: Fluorescence and magnetic resonance dual-modality imaging and photodynamic therapy in hepatocellular carcinoma. *Int. J. Nanomed.* **2019**, *14*, 57–74. [CrossRef] [PubMed]
74. Horcajada, P.; Chalati, T.; Serre, C.; Gillet, B.; Sebrie, C.; Baati, T.; Eubank, J.F.; Heurtaux, D.; Clayette, P.; Kreuz, C.; et al. Porous metal-organic-framework nanoscale carriers as a potential platform for drug deliveryand imaging. *Nat. Mater.* **2010**, *9*, 172–178. [CrossRef]
75. Wang, X.G.; Dong, Z.Y.; Cheng, H.; Wan, S.S.; Chen, W.H.; Zou, M.Z.; Huo, J.W.; Deng, H.X.; Zhang, X.Z. A multifunctional metal-organic framework based tumor targeting drug delivery system for cancer therapy. *Nanoscale* **2015**, *7*, 16061–16070. [CrossRef]
76. Mao, D.; Hu, F.; Kenry; Ji, S.; Wu, W.; Ding, D.; Kong, D.; Liu, B. Metal–Organic-Framework-Assisted In Vivo Bacterial Metabolic Labeling and Precise Antibacterial Therapy. *Adv. Mater.* **2018**, *30*, 1–7. [CrossRef]
77. Liu, F.; He, X.; Chen, H.; Zhang, J.; Zhang, H.; Wang, Z. Gram-scale synthesis of coordination polymer nanodots with renal clearance properties for cancer theranostic applications. *Nat. Commun.* **2015**, *6*, 1–9. [CrossRef]
78. Wang, D.; Zhou, J.; Chen, R.; Shi, R.; Xia, G.; Zhou, S.; Liu, Z.; Zhang, N.Q.; Wang, H.; Guo, Z.; et al. Magnetically guided delivery of DHA and Fe ions for enhanced cancer therapy based on pH-responsive degradation of DHA-loaded Fe_3O_4@C@MIL-100(Fe) nanoparticles. *Biomaterials* **2016**, *107*, 88–101. [CrossRef]
79. Liu, D.; He, C.; Poon, C.; Lin, W. Theranostic nanoscale coordination polymers for magnetic resonance imaging and bisphosphonate delivery. *J. Mater. Chem. B* **2014**, *2*, 8249–8255. [CrossRef]

80. Zhang, H.; Tian, X.T.; Shang, Y.; Li, Y.H.; Yin, X.B. Theranostic Mn-Porphyrin Metal-Organic Frameworks for Magnetic Resonance Imaging-Guided Nitric Oxide and Photothermal Synergistic Therapy. *ACS Appl. Mater. Interfaces* **2018**, *10*, 28390–28398. [CrossRef]
81. Qin, L.; Sun, Z.Y.; Cheng, K.; Liu, S.W.; Pang, J.X.; Xia, L.M.; Chen, W.H.; Cheng, Z.; Chen, J.X. Zwitterionic Manganese and Gadolinium Metal-Organic Frameworks as Efficient Contrast Agents for in Vivo Magnetic Resonance Imaging. *ACS Appl. Mater. Interfaces* **2017**, *9*, 41378–41386. [CrossRef] [PubMed]